The Ciliary Protein Arl13b Functions Outside of the Primary Cilium in Shh-Mediated Axon Guidance

Julien Ferent[1,2], **Sandii Constable**[3], **Eduardo D. Gigante**[3], **Patricia T. Yam**[1], **Laura E. Mariani**[3], **Emilie Legué**[4], **Karel F. Liem Jr.**[4], **Tamara Caspary**[3,7,*], **Frédéric Charron**[1,2,5,6,7,8,*]

[1]Montreal Clinical Research Institute (IRCM), 110 Pine Avenue West, Montreal, QC H2W 1R7, Canada

[2]Department of Neuroscience, University of Montreal, Montreal, QC H3T 1J4, Canada

[3]Department of Human Genetics, 615 Michael St., Suite 301, Emory University School of Medicine, Atlanta, GA 30322, USA

[4]Vertebrate Developmental Biology Program and Department of Pediatrics, Yale School of Medicine, 333 Cedar St., New Haven, CT 06520, USA

[5]Department of Anatomy and Cell Biology, Division of Experimental Medicine, McGill University, Montreal, QC H3A 0G4, Canada

[6]Department of Medicine, University of Montreal, Montreal, QC H3T 1J4, Canada

[7]These authors contributed equally

[8]Lead Contact

SUMMARY

The small GTPase Arl13b is enriched in primary cilia and regulates Sonic hedgehog (Shh) signaling. During neural development, Shh controls patterning and proliferation through a canonical, transcription-dependent pathway that requires the primary cilium. Additionally, Shh controls axon guidance through a non-canonical, transcription-independent pathway whose connection to the primary cilium is unknown. Here we show that inactivation of *Arl13b* results in defective commissural axon guidance *in vivo*. *In vitro*, we demonstrate that Arl13b functions autonomously in neurons for their Shh-dependent guidance response. We detect Arl13b protein in axons and growth cones, far from its well-established ciliary enrichment. To test whether Arl13b plays a non-ciliary function, we used an engineered, cilia-localization-deficient Arl13b variant and found that it was sufficient to mediate Shh axon guidance *in vitro* and *in vivo*. Together, these

*Correspondence: tcaspar@emory.edu (T.C.), frederic.charron@ircm.qc.ca (F.C.).

DECLARATION OF INTERESTS

The authors declare no competing interests.

results indicate that, in addition to its ciliary role in canonical Shh signaling, Arl13b plays a cilia-independent role in Shh-mediated axon guidance.

Graphical Abstract
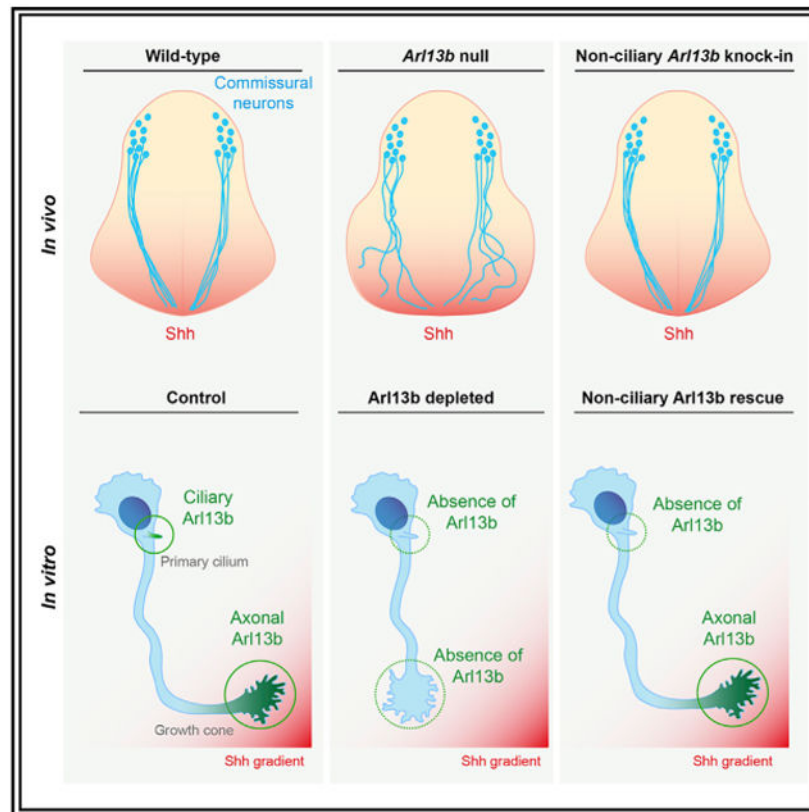
In Brief

Ciliary proteins such as Arl13b are crucial for canonical Shh signaling during neuronal development. Here, Ferent et al. investigate the role of Arl13b in non-canonical Shh signaling. They show that Arl13b is required for Shh-mediated axon guidance and that this role of Arl13b can be dissociated from its cilia localization.

INTRODUCTION

In the developing spinal cord, bone morphogenic proteins (BMPs) from the roof plate and Sonic hedgehog (Shh) from the floor plate form opposing gradients of activity that are essential to specify neurons (Ericson et al., 1997; Liem et al., 1997). Commissural neurons reside in the dorsal spinal cord and send axons ventrally. This is due to BMPs inducing repulsion through non-canonical signaling (Augsburger et al., 1999; Butler and Dodd, 2003). In addition, netrin1, produced by the ventricular zone and enriched along the pial edge in the dorsal spinal cord, confines axons to the periphery of the spinal cord (Dominici et al., 2017; Varadarajan et al., 2017). Subsequently, netrin1, Shh, and VEGF, produced by floor plate cells, cooperate to attract commissural axons at a distance and guide them to the ventral

midline (Charron et al., 2003; Kennedy et al., 1994; Moreno-Bravo et al., 2019; Ruiz de Almodovar et al., 2011; Serafini et al., 1994; Sloan et al., 2015; Wu et al., 2019).

Importantly, Shh is reused at multiple steps of neural development (Yam and Charron, 2013), including neural cell fate specification and axon guidance. Ventral neural cell fates are determined by a gradient of Shh activity, which is converted to a transcriptional response by the Gli family of transcription factors (Briscoe et al., 2000; Stamataki et al., 2005); this is referred to as the canonical Shh signaling pathway. In contrast, axon guidance by Shh occurs through a non-canonical transcription-independent pathway and relies on actin cytoskeleton remodeling at the growth cone (Lepelletier et al., 2017; Makihara et al., 2018; Yam et al., 2009, 2012).

Canonical Shh signaling is intimately linked to the primary cilium, a microtubule projection at the cell surface (Anvarian et al., 2019; Goetz and Anderson, 2010; Huangfu et al., 2003). Dynamic enrichment of Shh signaling components within cilia is critical both to activate Smoothened (Smo) and to process the Gli transcription factors that mediate the pathway's transcriptional response (Corbit et al., 2005; Haycraft et al., 2005; Huangfu and Anderson, 2005). Although axons are also microtubule-based cellular projections, the relationship between Shh signaling, the primary cilium, and axon guidance remains unexplored.

Joubert syndrome, a disease caused by mutations in more than 35 different cilia-associated genes, is diagnosed by the presence of a hindbrain malformation known as the molar tooth sign, a combination of the superior cerebellar peduncles failing to cross the midline of the brain and a hypoplastic cerebellum (Akizu et al., 2014; Doherty et al., 2013; Lee and Gleeson, 2011; Valente et al., 2013; Yachnis and Rorke, 1999). The patients also display abnormal pyramidal decussation and impaired crossing of the optic chiasm. Thus, Joubert syndrome patients exhibit defects in axon guidance although the mechanism underlying these defects is not known. One of the genes associated with Joubert syndrome is *ARL13B*, whose mouse ortholog *Arl13b* encodes a small GTPase highly enriched in cilia and that regulates canonical Shh signal transduction (Cantagrel et al., 2008; Caspary et al., 2007; Rafiullah et al., 2017; Thomas et al., 2015).

Although the mechanism of Arl13b is still unknown, Arl proteins are well established for their roles in trafficking. In the absence of Arl13b function, several components of Shh signaling are abnormally trafficked within cilia (Larkins et al., 2011). In normal conditions, in the absence of Shh ligand, Patched1 (Ptch1) is present at the ciliary membrane and the Gli proteins traffic in and out of the cilium, where they are cleaved to transcriptional repressors that shuttle to the nucleus (Haycraft et al., 2005; Huangfu and Anderson, 2005; Liu et al., 2005; Rohatgi et al., 2007). When Shh binds Ptch1, Ptch1 exits the cilium, and Smo becomes enriched at the cilium (Corbit et al., 2005; Rohatgi et al., 2007). The presence of activated Smo in the cilium leads to accumulation of Gli proteins at the tip of the cilium, inhibits Gli repressor (GliR) formation, and triggers the formation of Gli activator (GliA). In *Arl13b^{hnn/hnn}* mutant mouse embryos, cilia are short and the normal trafficking of Shh components to cilia is lost: Ptch1 and Smo are located in cilia regardless of the presence of Shh ligand, and there is no ligand-dependent Gli enrichment at the ciliary tip. The

consequence is that GliR production is normal, and there is low-level constitutive activation of the Shh transcriptional response (Caspary et al., 2007; Larkins et al., 2011).

In non-canonical Shh signaling, Shh guides axons by binding its receptor Boc, and possibly Ptch1, which localize to the growth cone (Ferent et al., 2019; Okada et al., 2006). This elicits two parallel downstream signaling activities: one that activates Smo, which in turn activates Src family kinases (SFKs) and initiates a cascade resulting in local β-actin protein synthesis, and another signaling activity that leads to the polarized activation of cytoskeletal actin remodeling proteins (Lepelletier et al., 2017; Makihara et al., 2018; Yam et al., 2009). These two processes, acting locally in the growth cone, result in growth cone turning toward Shh.

Given the role of Arl13b in canonical Shh signaling, we investigated whether Arl13b also plays a role in Shh-mediated axon guidance. Here we report abnormal commissural axon trajectory in embryos lacking Arl13b function. Despite abnormal neural patterning in *Arl13b* mutants, we show that mispatterning does not cause the abnormal commissural axon trajectory that we observe in *Arl13b* mutants, suggesting that Arl13b may act cell autonomously in axon guidance. Indeed, through *in vitro* turning assays, we demonstrate that Arl13b is required for commissural axon turning in response to Shh, indicating that Arl13b functions autonomously in commissural neurons, where it localizes to the growth cone. We further show that a cilia localization-deficient variant of Arl13b is sufficient to mediate axon turning toward Shh *in vitro*. *In vivo*, we show that knockin mice expressing a cilia localization-deficient Arl13b display normal commissural axon guidance. Together, these results establish that, in addition to its well-established ciliary role in canonical Shh signaling, Arl13b also has a cilia-independent role in Shh-mediated axon guidance.

RESULTS

Abnormal Commissural Axon Projections and Midline Crossing in *Arl13$^{hnn/hnn}$* Spinal Cord

To test whether Arl13b plays a role in commissural axon guidance, we analyzed embryonic day (E)11.5 *Arl13$^{hnn/hnn}$* (null) spinal cords using an antibody against Robo3. Robo3 marks commissural neurons from their cell bodies in the dorsal spinal cord through their axons projecting toward the floor plate and across the midline (Sabatier et al., 2004). As is routinely done to assess spinal commissural axon guidance, we performed our analysis on rostral sections, at the forelimb level. In E11.5 wild-type sections, commissural axons migrate along the periphery of the spinal cord until they reach the motor column (Figure 1A). At the motor column, commissural axons break away and dive toward the ventral midline, largely avoiding the motor column (Figure 1A). In *Arl13b$^{hnn/hnn}$* spinal cords, commissural axons migrate normally along the periphery of the spinal cord; however, upon reaching the motor column, many axons invade the motor column, and only a subset of axons reach the ventral midline (Figure 1B). We quantified the disorganization of Robo3+ axons in *Arl13b$^{hnn/hnn}$* ventral spinal cords by measuring the area of Robo3 staining relative to the total ventral area. *Arl13b$^{hnn/hnn}$* ventral spinal cords displayed a significant increase in the area occupied by Robo3+ axons compared to wild-type littermate controls (Figure 1C). Thus, *Arl13b$^{hnn/hnn}$* spinal cords display abnormal commissural axon projections and midline crossing.

Several mouse mutants of ciliary genes exhibit different degrees of severity of spinal cord mispatterning depending on axial position, with most showing profound defects in caudal neural tube patterning and normal or only slightly defective patterning of the rostral neural tube (Caspary et al., 2007; Eggenschwiler and Anderson, 2000; Huangfu and Anderson, 2005; Liem et al., 2009). Arl13b regulates Shh signaling during neural tube patterning, and *Arl13b^{hnn/hnn}* mutants have highly reduced levels of Shh in the caudal neural tube (Caspary et al., 2007), raising the possibility that the abnormal commissural axon projections in the *Arl13b^{hnn/hnn}* rostral spinal cord may be due to abnormal expression of Shh. To examine this, we stained rostral sections (i.e., at the same position where we analyzed Robo3+ axons) and caudal sections using an antibody against Shh. As expected in caudal sections, we detected Shh expression in the floor plate of control but significantly less in *Arl13b^{hnn/hnn}* sections (Figures 1D and 1E). In contrast, in rostral sections, we found normal Shh expression in the floor plate of both wild-type and *Arl13b^{hnn/hnn}* embryos. Together, these data suggest that the defect in axon guidance in *Arl13b^{hnn/hnn}* mutants is not due to abnormal expression of Shh in the floor plate. All subsequent analyses in this study were performed on rostral neural tube sections.

We next verified if the number of commissural neurons generated in *Arl13b^{hnn/hnn}* mutants is normal. For this, we quantified the number of Lhx2+ neurons (a marker of dI1 neurons and a transcription factor controlling directly *Robo3* expression) (Wilson et al., 2008). The number of Lhx2+ neurons in *Arl13b^{hnn/hnn}* mutants was not significantly different from controls (Figures S1A and S1B).

Neural Tube Mispatterning Does Not Cause the Abnormal Commissural Axon Trajectory Observed *Arl13b* Mutants

The commissural axon phenotype observed in *Arl13b^{hnn/hnn}* spinal cords could be due to a cell-autonomous role of Arl13b in commissural neurons or a non-cell-autonomous role of Arl13b in patterning the neural tube. Indeed, the motor column of embryos lacking Arl13b is expanded, reflecting a patterning defect (Caspary et al., 2007). Thus, to explore the possibility that the abnormal trajectory of commissural axons could be secondary to a patterning defect, we examined commissural axon guidance in Tubby-like protein 3 (Tulp3)-deficient embryos, which also display abnormal motor neuron patterning (Legue and Liem, 2019; Norman et al., 2009). Similar to Arl13b, Tulp3 is a cilia protein known to regulate Shh signaling and neural tube patterning. To determine whether Arl13b is expressed normally in the *Tulp3* mutant neural tube, we first analyzed forelimb-level E11.5 *Tulp3^{-/-}* (null) spinal cord sections with an Arl13b antibody. Using IFT88 as a cilium marker, we found that Arl13b localized normally to primary cilium in control and *Tulp3–/–* embryos (Figure 2A).

We next investigated whether Lhx2+ neurons are generated normally in *Tulp3* mutants. We observed that the number of Lhx2+ neurons in *Tulp3* mutants was not significantly different from controls (Figures S1C and S1D), indicating a normal patterning of commissural neurons in *Tulp3* mutants.

Following this, we investigated commissural axon trajectory in *Tulp3* mutants using an antibody against Robo3. In *Tulp3^{-/-}* spinal cords, compared to wild-type spinal cords, we observed that commissural axons projected normally for most of their trajectory, until they

came in close proximity to the floor plate, where we observed a small defasciculation of the axons (Figure 2B, arrows). Despite this small defasciculation, we found no difference when we measured the area of Robo3 staining relative to the total ventral area in wild-type and *Tulp3*$^{-/-}$ sections (Figure 2C). Thus, despite abnormal ventral neural patterning resembling *Arl13b* mutants, mispatterning on its own does not cause the abnormal motor column invasion by commissural axon that we observe in *Arl13b* mutants, suggesting that the commissural axon guidance defect observed in *Arl13b* mutants is unlikely to be due to a non-cell-autonomous role of Arl13b.

To further support these results, we next analyzed *Kif7* mutants for commissural axon guidance defects. *Kif7* mutants, analogously to *Arl13b* and *Tulp3* mutants, show an expansion of the motor column (Cheung et al., 2009). Robo3 immunostaining revealed that *Kif7* mutants did not show commissural axon guidance defects (Figures 2D and 2E). The absence of commissural axon guidance defects in *Kif7* mutants reinforces our *Tulp3* mutant results indicating that ventral cell fate mispatterning is not sufficient to cause the axon guidance defects observed in *Arl13b* mutants, supporting the idea that Arl13b functions in a cell-autonomous manner *in vivo* for commissural axon guidance.

Arl13b Is Required for Shh-Mediated Growth Cone Turning

Because the experiments above suggest that the role of Arl13b in commissural axons guidance is unlikely to be due to a non-cell-autonomous role in spinal cord patterning, we explored the possibility that Arl13 functions cell autonomously in the guidance of commissural neurons. Since Arl13b plays a role in canonical Shh signaling, we hypothesized that it might also play a role in Shh-signaling-mediated axon guidance of commissural axons. To test this, we first assessed the expression of Arl13b in commissural neurons. Using commissural neurons isolated from E13.5 rat spinal cords, we performed RNA sequencing (RNA-seq) and immunostaining. RNA-seq showed significant expression of *Arl13b* in commissural neurons, similar to the levels of *Boc* and *Smo* (Figure 3A). Immunostaining on commissural neurons cultured *in vitro* showed that Arl13b localizes to the primary cilium of commissural neurons, which is located at the cell body (Figure 3B). In addition, we detected a faint but reproducible amount of Arl13b present at the axon and the growth cone of commissural neurons. To confirm that this growth cone staining is indeed due to Arl13b, we electroporated commissural neurons with a short hairpin RNA (shRNA) against Arl13b (shArl13b) or a scrambled control and then performed Arl13b immunostaining. As expected, shArl13b significantly reduced the number of cilia that are Arl13b+ (Figures 3C and 3D). In addition, shArl13b significantly reduced growth cone Arl13b staining (Figures 3E and 3F), confirming the specificity of our growth cone Arl13b immunostaining. Thus, in addition to its ciliary localization, Arl13b is a bona fide growth cone protein.

Next, to assess whether Arl13b plays a role in Shh-mediated axon guidance of commissural axons, we turned to an *in vitro* system that enables us to measure axon turning in response to guidance cue gradients (Yam et al., 2009). We dissected commissural neurons from E13.5 rat spinal cords, electroporated them with either a scrambled shRNA or a shRNA against Arl13b, cultured them for 2 days, and exposed them to a Shh gradient in a Dunn chamber.

We imaged the axons and measured changes in trajectory in response to Shh; if the change in trajectory was a positive angle, the axon turned up the Shh gradient, whereas a negative angle indicated an axon turning down the Shh gradient. In commissural neurons electroporated with the scrambled shRNA, we found that axons did not turn significantly in the presence of a BSA control gradient, whereas they turned an average angle of ~30° toward a Shh gradient (Figures 3G and 3H). Interestingly, the knock down of Arl13b (using *Arl13b* shRNA) blocked the ability of commissural axons to turn toward Shh. These results indicate that Arl13b is required cell autonomously in commissural neurons for their Shh-dependent guidance response.

Cilia-Localization-Deficient Arl13b Is Sufficient for Shh-Mediated Growth Cone Turning

While we observed that Arl13b is highly enriched in the primary cilium of commissural neurons, we also found Arl13b, albeit at lower levels, present in axons and growth cones of commissural neurons (Figures 3B and 3E). The identification of a role for Arl13b in axon guidance, a process taking place at the level of the growth cone, raised the possibility of a novel, non-ciliary function of Arl13b. To directly assess whether the localization of Arl13b to the primary cilium is important for its role in axon guidance, we next used an Arl13b construct harboring a point mutation in the ciliary localization signal (Arl13b^{V358A}; Higginbotham et al., 2012; Mariani et al., 2016). While Arl13b-GFP localized strongly to the primary cilium, Arl13b^{V358A}-GFP did not localize to the primary cilium but was present in axons and growth cones of commissural neurons (Figure 4A). To test the importance of ciliary localization of Arl13b for axon guidance, we electroporated commissural neurons with either a scrambled shRNA or a shRNA against Arl13b, in the presence or absence of an Arl13b^{V358A} expression plasmid. As expected, neurons electroporated with scrambled shRNA showed attraction toward the Shh gradient (Figures 4B–4D). Knock down of Arl13b abolished the ability of commissural neurons to turn toward Shh. However, when we expressed Arl13b^{V358A} in Arl13b-deficient neurons, we observed that the turning response was completely restored. Together, these results indicate that localization of Arl13b to the primary cilium is not required for its role in axon guidance *in vitro*.

Commissural Axon Projections Are Normal in *Arl13b$^{V358A/V358A}$* Spinal Cord

To examine the impact of cilia-localization-deficient Arl13b on axon guidance *in vivo*, we generated knockin mice carrying the Arl13b^{V358A} variant (Gigante et al., 2019). We immunostained forelimb-level E11.5 sections of wild-type and *Arl13b$^{V358A/V358A}$* embryos for the ciliary marker IFT88. Primary cilia were still present in *Arl13b$^{V358A/V358A}$* embryos (Figure 4E). However, despite the Arl13b^{V358A} protein being expressed (Gigante et al., 2019) and the Arl13b antibody retaining the ability to recognize the Arl13b^{V358A} mutant protein (Figure S2), we detected no Arl13b^{V358A} protein in primary cilia (Figure 4E).

We next immunostained wild-type and *Arl13b$^{V358A/V358A}$* embryos with a Robo3 antibody to assess commissural axon trajectory. In E11.5 *Arl13b$^{V358A/V358A}$* embryos, we observed that commissural axons projected to the floor plate in a manner indistinguishable to wild-type embryos (Figure 4F). Indeed, we found no difference in the Robo3 staining area between wild-type and *Arl13b$^{V358A/V358A}$* embryos (Figure 4G), indicating that a

cilialocalization-deficient variant of Arl13b is sufficient to mediate commissural axon guidance.

DISCUSSION

Our data demonstrate that Arl13b is essential for Shh-dependent commissural axon guidance. Despite cilia being essential to transduce Shh-dependent neural cell fate specification and Arl13b being required for proper trafficking of Shh components within cilia, we found that the role of Arl13b in Shh-dependent axon guidance is cilia localization independent. Thus, Arl13b regulates Shh signaling through two mechanisms: a cilia-associated one to specify cell fate and a cilia-localization-independent one to guide axons.

The *in vivo* axon guidance phenotype that we observed in *Arl13b* mutants has similarities with the phenotype that we have observed in mouse mutants of the Shh axon guidance signaling pathway, such as *Boc* mutants (Okada et al., 2006) and *Smo* conditional mutants (Charron et al., 2003). The motor column invasion phenotype reflects a defect in long-range commissural axon attraction to the midline. In wild-type conditions, Shh attracts commissural axons over the last few hundred micrometers through the ventral spinal cord, ensuring that the axons' growth is strongly directed to the ventral midline. When Shh attraction is impaired, some axons now invade the motor column and appear to defasciculate from the main axon bundle. Interestingly, the loss of Arl13b impacts commissural axon guidance more severely than the inactivation of *Boc* or the conditional inactivation of *Smo* (Charron et al., 2003; Okada et al., 2006). Thus, loss of Arl13b has a stronger commissural axon phenotype than loss of Shh-mediated axon guidance alone. This could be due to Arl13b also having—in addition to its cell autonomous role—a non-cell-autonomous role in commissural axon guidance. However, the fact that we do not see the same extent of commissural axon guidance defects in two other mutants (*Tulp3*^{-/-} and *Kif7*^{-/-}) harboring neural tube defects similar to *Arl13b* mutants suggests that, on their own, these patterning defects are not sufficient to cause the strong invasion of the motor column observed in *Arl13b* mutants. Nonetheless, we cannot exclude that there might be a relatively minor non-cell-autonomous contribution of Arl13b in commissural axon guidance, in addition to its cell-autonomous role.

Another non-mutually exclusive possibility to explain that loss of Arl13b has a stronger commissural axon phenotype than loss of Shh-mediated axon guidance alone is that Arl13b might be required for other commissural axon guidance cues besides Shh, such as netrin1 or VEGF. In addition to motor column invasion, we also observed that fewer commissural axons reach the ventral midline in *Arl13b* mutants compared to controls. The reason for the reduction in the number of axons reaching the floor plate and thus forming a thinner commissure is unknown. Intriguingly, a reduction in commissure thickness is also observed in a mouse mutant that harbors a floor plate deletion of *netrin1* (Wu et al., 2019). Thus, one possibility is that Arl13b is also important for netrin1-mediated axon guidance. Additional work will be required to determine whether this is the case.

Shh in Axon Guidance versus Cell Migration and Cell-type-Specific Roles for Arl13b

Shh controls axon guidance by binding the receptor Boc, and possibly Ptch1, which localize to the growth cone (Ferent et al., 2019; Okada et al., 2006). Shh binding elicits two parallel downstream signaling activities: (1) it activates the signal transducer Smo, which in turn activates Src family kinases and initiates a cascade resulting in local actin protein synthesis, and (2) it leads to the polarized activation of cytoskeletal actin remodeling proteins, resulting in growth cone turning toward the Shh source (Lepelletier et al., 2017; Makihara et al., 2018; Yam et al., 2009). Because these effects occur locally at the growth cone, independently of Gli-mediated transcription, they are unlikely to require the primary cilium, which is located far back at the cell body. In fact, growth cone turning can take place even if the cell body of the neuron is severed from the axon, indicating that, at least for some guidance cues, this process does not require the cilium to be present (Harris et al., 1987). Consistent with this, by expressing the cilia-localization-deficient Arl13b variant *in vitro* and *in vivo*, our data show that Arl13b, despite its robust normal association with the cilium, functions outside the cilium to control axon guidance.

Another Shh-dependent phenomenon that is transcription independent is fibroblast migration in response to Shh. *In vitro*, fibroblasts migrate toward a Shh source, and this is disrupted by mutations in *Ptch1*, *Smo*, or *Arl13b* (Bijlsma et al., 2012; Mariani et al., 2016). Moreover, a cilia-localization-deficient Arl13b variant is not able to support the migration of fibroblasts toward Shh (Mariani et al., 2016). This contrasts sharply with our results where Arl13b localization to cilia is not required for Shh-mediated commissural axon guidance. One distinction between the two situations is the distance of the primary cilium to the leading edge of migration. In the case of fibroblasts, the primary cilium is very close to the migratory leading edge; however, in neurons, the primary cilium is much further away from the growth cone. Whether this distance plays a role in the requirement for cilium in migration versus guidance remains to be determined. Regardless, this highlights a fundamental difference in the requirement for the localization of Arl13b in cell migration versus axon guidance.

In addition to fibroblasts, Arl13b is also critical for interneuron migration during cortical development (Higginbotham et al., 2012). Similar to fibroblast migration in response to Shh, the cilia-localization-deficient Arl13b variant does not rescue Arl13b-deficient interneuron migration. Although Shh affects the motility of interneurons, it remains to be determined whether Shh acts as a guidance cue for these cells (Baudoin et al., 2012). Nonetheless, these results indicate that cell migration and axon guidance have a differential localization requirement for Arl13b.

Do Joubert Syndrome Arl13b Mutants Have Altered Neuronal Localization?

Altered Arl13b subcellular localization might underly the pathological effect of some *Arl13b* mutations in Joubert syndrome. To investigate whether Arl13b mutants that are associated with Joubert syndrome have an altered neuronal localization, we have looked at the three missense Arl13b mutations described so far to be causal for Joubert syndrome (Cantagrel et al., 2008; Thomas et al., 2015). We expressed GFP fusions of Arl13b[WT], Arl13b[Y86C], Arl13b[R79Q], and Arl13b[R200C] in dissociated commissural neurons (Figure S3).

Although all of them are expressed in cell lines (data not shown), not all of them are expressed in commissural neurons (Arl13b^{Y86C} and Arl13b^{R200C}). In addition, Arl13b^{R79Q}, which still localizes to the primary cilium, also localizes abundantly to the growth cone (arrow). Further investigations will be required to assess how this change in localization might impact function.

A Molecular Mechanism for the Axon Guidance Defects of Joubert Syndrome Patients?

More than 35 genes have thus far been associated with Joubert syndrome; all of them encode proteins that localize to the cilium or centrosome (Doherty et al., 2013). The primary diagnostic criterion for Joubert syndrome is the molar tooth sign, a malformation that involves abnormal white matter tracts projecting from the cerebellum. In addition, Joubert syndrome patients display other phenotypes reflecting axon guidance defects, including problems with axonal midline crossing at the pyramidal decussation and the optic chiasm. Because Shh is an axon guidance cue at the optic chiasm (Fabre et al., 2010; Peng et al., 2018), we speculate that the cilia-associated genes mutated in Joubert syndrome might disrupt Shh-mediated axon guidance in addition to disrupting canonical Shh signaling.

In conclusion, our data argue that at least one cilia-associated protein, Arl13b, plays a non-ciliary role in axon guidance. It will be interesting to determine whether the other Joubert-syndrome-associated proteins do the same.

STAR★METHODS

LEAD CONTACT AND MATERIALS AVAILABILITY

Further information and requests for resources and reagents should be directed to and will be fulfilled by the Lead Contact, Frédéric Charron (frederic.charron@ircm.qc.ca). All unique reagents generated in this study are available from the Lead Contact without restriction.

EXPERIMENTAL MODEL AND SUBJECT DETAILS

Animals—All mouse work was performed under the approved guidelines of the Emory University, Yale University Institutional Animal Care and Use Committees, or Canadian Council on Animal Care Guidelines (and approved by the IRCM Animal Care Committee); rat work was performed in accordance with the Canadian Council on Animal Care Guidelines and was approved by the IRCM Animal Care Committee. Staged pregnant Sprague Dawley rats were obtained from Charles River (St. Constant, Canada). Mouse strains used were: *Arl13b$^{hnn/hnn}$* (MGI:3578151), *Arl13b^{V358A}* (MGI:6256969, official nomenclature *Arl13b^{em1Tc}*)(Gigante et al., 2019), *Kif7* (MGI:4357956, *Kif7tm1.2Hui*) (Cheung et al., 2009), *Tulp3$^{-/-}$* (MGI: 5548429 *Tulp3$^{tm1b(EUCOMM)hmgu}$*) (Legue and Liem, 2019). All mouse embryos were used at embryonic day 11.5 (E11.5), as indicated in the Results section and in the figure legends. Rat embryos were used at E13. Male and female embryos were used. Genotyping was performed as previously described for *Arl13b$^{hnn/hnn}$* (Caspary et al., 2007). *Arl13b^{V358A}* PCR genotyping used primers: V358AF – GAATGAAAAGGAGTCAGCGGG and V358AR – TGAACCGCTAATGGGA AACT, which yields a ~200 bp wild-type product. The product is cut to 179bp by Cac8I restriction enzyme on the *Arl13b^{V358A}* mutant allele.

METHOD DETAILS

Primary Commissural Neuron Culture—Dissociated commissural neuron cultures were prepared as previously described (Langlois et al., 2010; Yam et al., 2009). Briefly, tissue culture plates or acid-washed and sterilized glass coverslips were coated with PLL (100 μg/ml for 2 h). The dorsal fifth of E13 rat neural tubes were microdissected and quickly washed once in cold Ca^{2+}/Mg2+-free HBSS. The neural tube sections were trypsinized in 0.15% trypsin in Ca^{2+}/Mg2+-free HBSS for 7 min at 37°C. DNase was added for 15 s. The tissue fragments were then washed in warm Ca^{2+}/Mg2+-free HBSS and triturated in Ca^{2+}/Mg2+-free HBSS to yield a suspension of single cells. Cells were plated in Neurobasal media supplemented with 10% heat-inactivated FBS and 2 mM GlutaMAX. After ~21 h, the medium was changed to Neurobasal supplemented with 2% B27 and 2 mM GlutaMAX. Commissural neurons were used for experiments ~48 h after plating.

shRNA Generation and Evaluation—The target sequence for rat Arl13b was identified using BLOCK-iT™ RNAi Designer (Thermo Fisher Scientific): 5′-TGTGATGGTCGGACTTGATAA –3′.

shRNA target sequence with a microRNA stem (shRNAmir) for knockdown of Arl13b was generated by ligating oligonucleotides encoding the target sequences into the pcDNA6.2-GW/EmGFP-miR vector. The shRNA/miR/EmGFP sequence was then cloned via attB/attP site recombination (using BP clonase) into the pDONR221 backbone (ThermoFisher, 12536-017), and via attL/attR site recombination (using LR clonase) into a custom expression vector derived from Gateway pcDNA-DEST47 (ThermoFisher Scientific, 12281-010). This custom expression vector replaced the promoter and polyA regions of Gateway pcDNA-DEST47 with the promoter and polyA from the pCAGGS vector (Stühmer et al., 2002) to improve its expression in mammalian neurons. The efficiency and specificity of this shRNAs was evaluated *in vitro* by immunofluorescence.

shRNA-Resistant Arl13b^{V358A} Expression Vectors—To perform rescue experiments, we used mouse *Arl13b^{V358A}* mutant sequence cloned into the pCAGGS vector for neuronal expression. The mouse sequence is impervious to the rat Arl13b shRNA.

Arl13b Expression Vectors with Joubert Syndrome Mutations—We cloned wild-type Arl13b, Arl13b^{Y86C}, Arl13b^{R79Q} and Arl13b^{R200C} into the pCAGGS vector in frame with GFP for neuronal expression.

Growth Cone Turning Assays—Commissural neurons were electroporated with the Amaxa 96-well Shuttle using the Primary Cell 96-well Nucleofector Kit (Lonza, Switzerland) according to the manufacturer's instructions. For each electroporation in one well of a 96-well Nucleofector Plate, $3\text{-}5 \times 10^5$ cells and 0.6 μg plasmid DNA was used. The electroporation was performed with the program 96-DC-100. In parallel to shArl13b, neurons were treated with a scrambled shRNA control. For Dunn chamber axon guidance assays, primary neurons were grown on PLL-coated square #3D coverslips (Fisher Scientific) at low density. After Dunn chamber assembly, timelapse phase contrast images were acquired for a minimum of 2 hr. Gradients were generated with 0.1 μg/ml recombinant

human Shh, or buffer containing BSA (the vehicle for Shh) as the control in the outer well. The angle turned was defined as the angle between the original direction of the axon and a straight line connecting the base of the growth cone from the first to the last time point of the assay period. For details, see Yam et al. (2009).

In Vivo Commissural Axon Staining—Immunofluorescence was performed using standard protocols on E11.5 embryonic spinal cords fixed for 1-1/2 hours in 4% PFA in PBS at 4°C, washed 3 times in PBS, then transferred to 30% sucrose in 0.1% phosphate buffer overnight before embedding in OCT and cryosectioning at 14-18 μm. Samples were blocked for 1hr in 10% horse or donkey serum in PBS containing 0.1% Triton X-100. Primary antibodies listed were incubated overnight at 4°C. Anti-Robo3 (1:500, R&D Systems AF3076), anti-Shh (1:20, Developmental Studies Hybridoma Bank, 5E1), rabbit polyclonal anti-Arl13b (1:2000) (Caspary et al., 2007), anti-Arl13b (1:2000, NeuroMab N295B/66), anti-IFT88 (kind gift from Brad Yoder), and anti-Lhx2 (1:100, Developmental Studies Hybridoma Bank, PCRP-LHX2-1C11). Secondary antibodies were conjugated to Alexa Fluor 488, 568 or 594 (1:1000, Thermo Fisher). Nuclei were visualized with DAPI nuclear dye (1:500, Sigma) added with the secondary antibodies. Sections were mounted in Prolong Gold (Thermo Fisher, P36934) or Mowiol (Calbiochem).

Imaging and Quantification—Images were acquired on Leica SP8 multiphoton confocal microscope. Multiple high-magnification images of the neural tube were taken and stitched using confocal software to form a complete image. Stitched images were false colored and inverted using FIJI.

To quantify the relative Robo3+ area, we measured the neural tube along the ventro-dorsal axis and divided the neural tube into two halves: a dorsal half and a ventral half. We then measured the area occupied by Robo3+ axons relative to the ventral area.

QUANTIFICATION AND STATISTICAL ANALYSIS

Statistical analyses were performed with GraphPad Prism 5 (La Jolla, CA). Student's t test or Mann-Whitney test were used when there were two groups in the dataset. To compare multiple groups in a dataset, one-way ANOVA was used. The statistical analysis used in each experiment and the definition of n are stated in the figure legends.

DATA AND CODE AVAILABILITY

This study did not generate any unique datasets or code.

Supplementary Material

Refer to Web version on PubMed Central for supplementary material.

ACKNOWLEDGMENTS

REFERENCES

Akizu N, Silhavy JL, Rosti RO, Scott E, Fenstermaker AG, Schroth J, Zaki MS, Sanchez H, Gupta N, Kabra M, et al. (2014). Mutations in CSPP1 lead to classical Joubert syndrome. Am. J. Hum. Genet 94, 80–86. [PubMed: 24360807]

Anvarian Z, Mykytyn K, Mukhopadhyay S, Pedersen LB, and Christensen ST (2019). Cellular signalling by primary cilia in development, organ function and disease. Nat. Rev. Nephrol 15, 199–219. [PubMed: 30733609]

Augsburger A, Schuchardt A, Hoskins S, Dodd J, and Butler S (1999). BMPs as mediators of roof plate repulsion of commissural neurons. Neuron 24, 127–141. [PubMed: 10677032]

Baudoin JP, Viou L, Launay PS, Luccardini C, Espeso Gil S, Kiyasova V, Irinopoulou T, Alvarez C, Rio JP, Boudier T, et al. (2012). Tangentially migrating neurons assemble a primary cilium that promotes their reorientation to the cortical plate. Neuron 76, 1108–1122. [PubMed: 23259947]

Bijlsma MF, Damhofer H, and Roelink H (2012). Hedgehog-stimulated chemotaxis is mediated by smoothened located outside the primary cilium. Sci. Signal 5, ra60. [PubMed: 22912493]

Briscoe J, Pierani A, Jessell TM, and Ericson J (2000). A homeodomain protein code specifies progenitor cell identity and neuronal fate in the ventral neural tube. Cell 101, 435–45. [PubMed: 10830170]

Butler SJ, and Dodd J (2003). A role for BMP heterodimers in roof plate-mediated repulsion of commissural axons. Neuron 38, 389–401. [PubMed: 12741987]

Cantagrel V, Silhavy JL, Bielas SL, Swistun D, Marsh SE, Bertrand JY, Audollent S, Attié-Bitach T, Holden KR, Dobyns WB, et al.; International Joubert Syndrome Related Disorders Study Group (2008). Mutations in the cilia gene ARL13B lead to the classical form of Joubert syndrome. Am. J. Hum. Genet 83, 170–179. [PubMed: 18674751]

Caspary T, Larkins CE, and Anderson KV (2007). The graded response to Sonic Hedgehog depends on cilia architecture. Dev. Cell 12, 767–778. [PubMed: 17488627]

Charron F, Stein E, Jeong J, McMahon AP, and Tessier-Lavigne M (2003). The morphogen sonic hedgehog is an axonal chemoattractant that collaborates with netrin-1 in midline axon guidance. Cell 113,11–23. [PubMed: 12679031]

Cheung HO, Zhang X, Ribeiro A, Mo R, Makino S, Puviindran V, Law KK, Briscoe J, and Hui CC (2009). The kinesin protein Kif7 is a critical regulator of Gli transcription factors in mammalian hedgehog signaling. Sci. Signal 2, ra29. [PubMed: 19549984]

Corbit KC, Aanstad P, Singla V, Norman AR, Stainier DY, and Reiter JF (2005). Vertebrate Smoothened functions at the primary cilium. Nature 437, 1018–1021. [PubMed: 16136078]

Doherty D, Millen KJ, and Barkovich AJ (2013). Midbrain and hindbrain malformations: advances in clinical diagnosis, imaging, and genetics. Lancet Neurol. 12, 381–393. [PubMed: 23518331]

Dominici C, Moreno-Bravo JA, Puiggros SR, Rappeneau Q, Rama N, Vieugue P, Bernet A, Mehlen P, and Chédotal A (2017). Floor-plate-derived netrin-1 is dispensable for commissural axon guidance. Nature 545, 350–354. [PubMed: 28445456]

Eggenschwiler JT, and Anderson KV (2000). Dorsal and lateral fates in the mouse neural tube require the cell-autonomous activity of the open brain gene. Dev. Biol 227, 648–660. [PubMed: 11071781]

Ericson J, Briscoe J, Rashbass P, van Heyningen V, and Jessell TM (1997). Graded sonic hedgehog signaling and the specification of cell fate in the ventral neural tube. Cold Spring Harb. Symp. Quant. Biol 62, 451–466. [PubMed: 9598380]

Fabre PJ, Shimogori T, and Charron F (2010). Segregation of ipsilateral retinal ganglion cell axons at the optic chiasm requires the Shh receptor Boc. J. Neurosci 30, 266–275. [PubMed: 20053908]

Ferent J, Giguere F, Jolicoeur C, Morin S, Michaud JF, Makihara S, Yam PT, Cayouette M, and Charron F (2019). Boc Acts via Numb as a Shh-Dependent Endocytic Platform for Ptch1 Internalization and Shh-Mediated Axon Guidance. Neuron 102, 1157–1171.e5. [PubMed: 31054872]

Gigante ED, Taylor MR, Ivanova AA, Kahn RA, and Caspary T (2019). Arl13b regulates Sonic Hedgehog signaling from outside primary cilia. bio-Rxiv,. 10.1101/711671.

Goetz SC, and Anderson KV (2010). The primary cilium: a signalling centre during vertebrate development. Nat. Rev. Genet 11, 331–344. [PubMed: 20395968]

Harris WA, Holt CE, and Bonhoeffer F (1987). Retinal axons with and without their somata, growing to and arborizing in the tectum of Xenopus embryos: a time-lapse video study of single fibres in vivo. Development 101, 123–133. [PubMed: 3449363]

Haycraft CJ, Banizs B, Aydin-Son Y, Zhang Q, Michaud EJ, and Yoder BK (2005). Gli2 and Gli3 localize to cilia and require the intraflagellar transport protein polaris for processing and function. PLoS Genet. 1, e53. [PubMed: 16254602]

Higginbotham H, Eom TY, Mariani LE, Bachleda A, Hirt J, Gukassyan V, Cusack CL, Lai C, Caspary T, and Anton ES (2012). Arl13b in primary cilia regulates the migration and placement of interneurons in the developing cerebral cortex. Dev. Cell 23, 925–938. [PubMed: 23153492]

Huangfu D, and Anderson KV (2005). Cilia and Hedgehog responsiveness in the mouse. Proc. Natl. Acad. Sci. USA 102, 11325–11330. [PubMed: 16061793]

Huangfu D, Liu A, Rakeman AS, Murcia NS, Niswander L, and Anderson KV (2003). Hedgehog signalling in the mouse requires intraflagellar transport proteins. Nature 426, 83–87. [PubMed: 14603322]

Kennedy TE, Serafini T, de la Torre JR, and Tessier-Lavigne M (1994). Netrins are diffusible chemotropic factors for commissural axons in the embryonic spinal cord. Cell 78, 425–35. [PubMed: 8062385]

Langlois SD, Morin S, Yam PT, and Charron F (2010). Dissection and culture of commissural neurons from embryonic spinal cord. J. Vis. Exp 2010, 1773.

Larkins CE, Aviles GD, East MP, Kahn RA, and Caspary T (2011). Arl13b regulates ciliogenesis and the dynamic localization of Shh signaling proteins. Mol. Biol. Cell 22, 4694–4703. [PubMed: 21976698]

Lee JE, and Gleeson JG (2011). Cilia in the nervous system: linking cilia function and neurodevelopmental disorders. Curr. Opin. Neurol 24, 98–105. [PubMed: 21386674]

Legue E, and Liem KF Jr. (2019). Tulp3 Is a Ciliary Trafficking Gene that Regulates Polycystic Kidney Disease. Curr. Biol 29, 803–812.e5. [PubMed: 30799240]

Lepelletier L, Langlois SD, Kent CB, Welshhans K, Morin S, Bassell GJ, Yam PT, and Charron F (2017). Sonic Hedgehog Guides Axons via Zipcode Binding Protein 1-Mediated Local Translation. J. Neurosci 37, 1685–1695. [PubMed: 28073938]

Liem KF Jr., Tremml G, and Jessell TM (1997). A role for the roof plate and its resident TGFbeta-related proteins in neuronal patterning in the dorsal spinal cord. Cell 91, 127–138. [PubMed: 9335341]

Liem KF Jr., He M, Ocbina PJ, and Anderson KV (2009). Mouse Kif7/Costal2 is a cilia-associated protein that regulates Sonic hedgehog signaling. Proc. Natl. Acad. Sci. USA 106, 13377–13382. [PubMed: 19666503]

Liu A, Wang B, and Niswander LA (2005). Mouse intraflagellar transport proteins regulate both the activator and repressor functions of Gli transcription factors. Development 132, 3103–3111. [PubMed: 15930098]

Makihara S, Morin S, Ferent J, Cote JF, Yam PT, and Charron F (2018). Polarized Dock Activity Drives Shh-Mediated Axon Guidance. Dev. Cell 46, 410–25.e7. [PubMed: 30078728]

Mariani LE, Bijlsma MF, Ivanova AA, Suciu SK, Kahn RA, and Caspary T (2016). Arl13b regulates Shh signaling from both inside and outside the cilium. Mol. Biol. Cell 27, 3780–3790.

Moreno-Bravo JA, Roig Puiggros S, Mehlen P, and Chédotal A (2019). Synergistic Activity of Floor-Plate- and Ventricular-Zone-Derived Netrin-1 in Spinal Cord Commissural Axon Guidance. Neuron 101, 625–634.e3. [PubMed: 30661739]

Norman RX, Ko HW, Huang V, Eun CM, Abler LL, Zhang Z, Sun X, and Eggenschwiler JT (2009). Tubby-like protein 3 (TULP3) regulates patterning in the mouse embryo through inhibition of Hedgehog signaling. Hum. Mol. Genet 18, 1740–1754. [PubMed: 19286674]

Okada A, Charron F, Morin S, Shin DS, Wong K, Fabre PJ, Tessier-Lavigne M, and McConnell SK (2006). Boc is a receptor for sonic hedgehog in the guidance of commissural axons. Nature 444, 369–373. [PubMed: 17086203]

Peng J, Fabre PJ, Dolique T, Swikert SM, Kermasson L, Shimogori T, and Charron F (2018). Sonic Hedgehog Is a Remotely Produced Cue that Controls Axon Guidance Trans-axonally at a Midline Choice Point. Neuron 97, 326–340.e4. [PubMed: 29346753]

Rafiullah R, Long AB, Ivanova AA, Ali H, Berkel S, Mustafa G, Paramasivam N, Schlesner M, Wiemann S, Wade RC, et al. (2017). A novel homozygous ARL13B variant in patients with Joubert syndrome impairs its guanine nucleotide-exchange factor activity. Eur. J. Hum. Genet 25, 1324–1334. [PubMed: 29255182]

Rohatgi R, Milenkovic L, and Scott MP (2007). Patched1 regulates hedgehog signaling at the primary cilium. Science 317, 372–376. [PubMed: 17641202]

Ruiz de Almodovar C, Fabre PJ, Knevels E, Coulon C, Segura I, Haddick PC, Aerts L, Delattin N, Strasser G, Oh WJ, et al. (2011). VEGF mediates commissural axon chemoattraction through its receptor Flk1. Neuron 70, 966–978. [PubMed: 21658588]

Sabatier C, Plump AS, Le Ma, Brose K, Tamada A, Murakami F, Lee EY, and Tessier-Lavigne M (2004). The divergent Robo family protein rig-1/Robo3 is a negative regulator of slit responsiveness required for midline crossing by commissural axons. Cell 117, 157–169. [PubMed: 15084255]

Serafini T, Kennedy TE, Galko MJ, Mirzayan C, Jessell TM, and Tessier-Lavigne M (1994). The netrins define a family of axon outgrowth-promoting proteins homologous to C. elegans UNC-6. Cell 78, 409–424. [PubMed: 8062384]

Sloan TF, Qasaimeh MA, Juncker D, Yam PT, and Charron F (2015). Integration of shallow gradients of Shh and Netrin-1 guides commissural axons. PLoS Biol. 13, e1002119. [PubMed: 25826604]

Stamataki D, Ulloa F, Tsoni SV, Mynett A, and Briscoe J (2005). A gradient of Gli activity mediates graded Sonic Hedgehog signaling in the neural tube. Genes Dev. 19, 626–641. [PubMed: 15741323]

Stühmer T, Anderson SA, Ekker M, and Rubenstein JL (2002). Ectopic expression of the Dlx genes induces glutamic acid decarboxylase and Dlx expression. Development 129, 245–252. [PubMed: 11782417]

Thomas S, Cantagrel V, Mariani L, Serre V, Lee JE, Elkhartoufi N, de Lonlay P, Desguerre I, Munnich A, Boddaert N, et al. (2015). Identification of a novel ARL13B variant in a Joubert syndrome-affected patient with retinal impairment and obesity. Eur. J. Hum. Genet 23, 621–627. [PubMed: 25138100]

Valente EM, Dallapiccola B, and Bertini E (2013). Joubert syndrome and related disorders. Handb. Clin. Neurol 113, 1879–1888. [PubMed: 23622411]

Varadarajan SG, Kong JH, Phan KD, Kao TJ, Panaitof SC, Cardin J, Eltzschig H, Kania A, Novitch BG, and Butler SJ (2017). Netrin1 Produced by Neural Progenitors, Not Floor Plate Cells, Is Required for Axon Guidance in the Spinal Cord. Neuron 94, 790–799.e3. [PubMed: 28434801]

Wilson SI, Shafer B, Lee KJ, and Dodd J (2008). A molecular program for contralateral trajectory: Rig-1 control by LIM homeodomain transcription factors. Neuron 59, 413–24. [PubMed: 18701067]

Wu Z, Makihara S, Yam PT, Teo S, Renier N, Balekoglu N, Moreno-Bravo JA, Olsen O, Chédotal A, Charron F, and Tessier-Lavigne M (2019). Long-Range Guidance of Spinal Commissural Axons by Netrin1 and Sonic Hedgehog from Midline Floor Plate Cells. Neuron 101, 635–647.e4. [PubMed: 30661738]

Yachnis AT, and Rorke LB (1999). Neuropathology of Joubert syndrome. J. Child Neurol 14, 655–659, discussion 669–672. [PubMed: 10511338]

Yam PT, and Charron F (2013). Signaling mechanisms of non-conventional axon guidance cues: the Shh, BMP and Wnt morphogens. Curr. Opin. Neurobiol 23, 965–973. [PubMed: 24183376]

Yam PT, Langlois SD, Morin S, and Charron F (2009). Sonic hedgehog guides axons through a noncanonical, Src-family-kinase-dependent signaling pathway. Neuron 62, 349–362. [PubMed: 19447091]

Yam PT, Kent CB, Morin S, Farmer WT, Alchini R, Lepelletier L, Colman DR, Tessier-Lavigne M, Fournier AE, and Charron F (2012). 14-3-3 proteins regulate a cell-intrinsic switch from sonic hedgehog-mediated commissural axon attraction to repulsion after midline crossing. Neuron 76, 735–749. [PubMed: 23177959]

Highlights

- *Arl13b* null mutant mice display commissural axon guidance defects

- Arl13b is required for Shh-mediated growth cone attraction

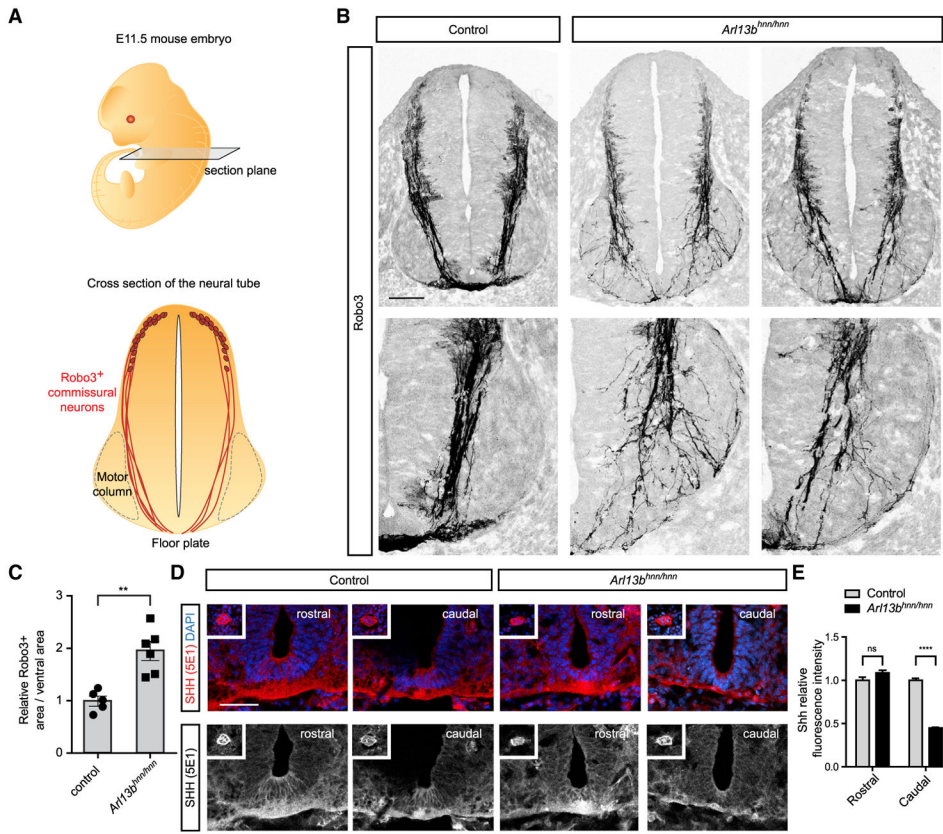- Cilia-deficient Arl13b is sufficient for its role in axon guidance

Figure 1. Abnormal Commissural Axon Projections and Midline Crossing in *Arl13b^hnn/hnn* Spinal Cord

(A) Schematic of an E11.5 embryo and cross-section of the neural tube at the forelimb level. Sections are labeled with Robo3, which marks commissural axons projecting from the dorsal neural tube to the floor plate.

(B) Robo3 immunostaining of E11.5 spinal cord cross-sections of *Arl13b^hnn/hnn* mice.

(C) The area occupied by Robo3+ axons relative to the total area of the ventral neural tube (mean ± SEM) is significantly higher in *Arl13b^hnn/hnn* mice compared to control mice (t test, **p < 0.01).

(D) Shh immunostaining of E11.5 rostral spinal cord cross-sections. Inset shows the notochord.

(E) The Shh relative fluorescence intensity is quantified at both rostral and caudal levels (mean ± SEM). Two-way ANOVA, Bonferroni multiple comparisons (****p < 0.0001). Number of embryos: 5 *Arl13b^hnn/hnn*; 6 control; and 3 sections per embryo.

Scale bars: 100 μm (B) and 50 μm (D).
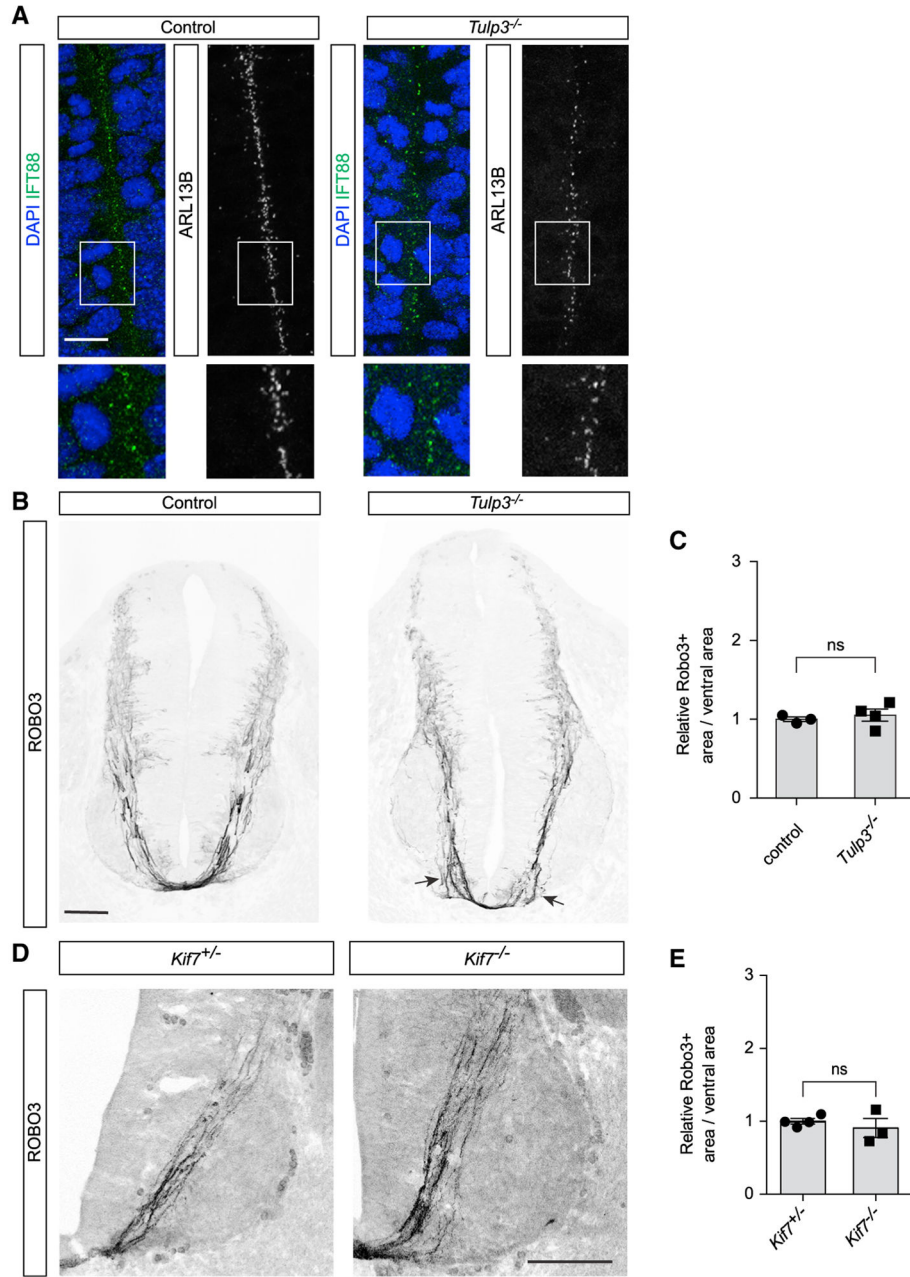
See also Figure S1.

Figure 2. Neural Tube Mispatterning Does Not Cause the Abnormal Commissural Axon Trajectory Observed *Arl13b^hnn/hnn* Mutants

(A) IFT88 and Arl13b co-immunostaining of E11.5 spinal cord cross-sections in *Tulp3^−/−* and control mice.

(B) Robo3 immunostaining of E11.5 spinal cord cross-sections of *Tulp3^−/−* mice. Some defasciculating axons are noticeable near the floor plate in *Tulp3^−/−* mice (arrows).

(C) Quantification of the area occupied by Robo3+ axons relative to the total area of the ventral neural tube (mean ± SEM) in *Tulp3^−/−* mice compared to control mice (t test). Number of embryos: 4 *Tulp3^−/−*; 3 control; and 2 sections per embryo.

(D) Robo3 immunostaining of E11.5 *Kif7^−/−* spinal cord cross-sections.

(E) Quantification of the area occupied by Robo3+ axons relative to the total area of the ventral neural tube (mean ± SEM) in *Kif7*^{−/−} compared to *Kif7*^{+/−} mice (t test). Number of embryos: 4 *Kif7*^{−/−} and 3 *Kif7*^{+/−}.

Scale bars: 10 μm (A) and 100 μm (B and D).
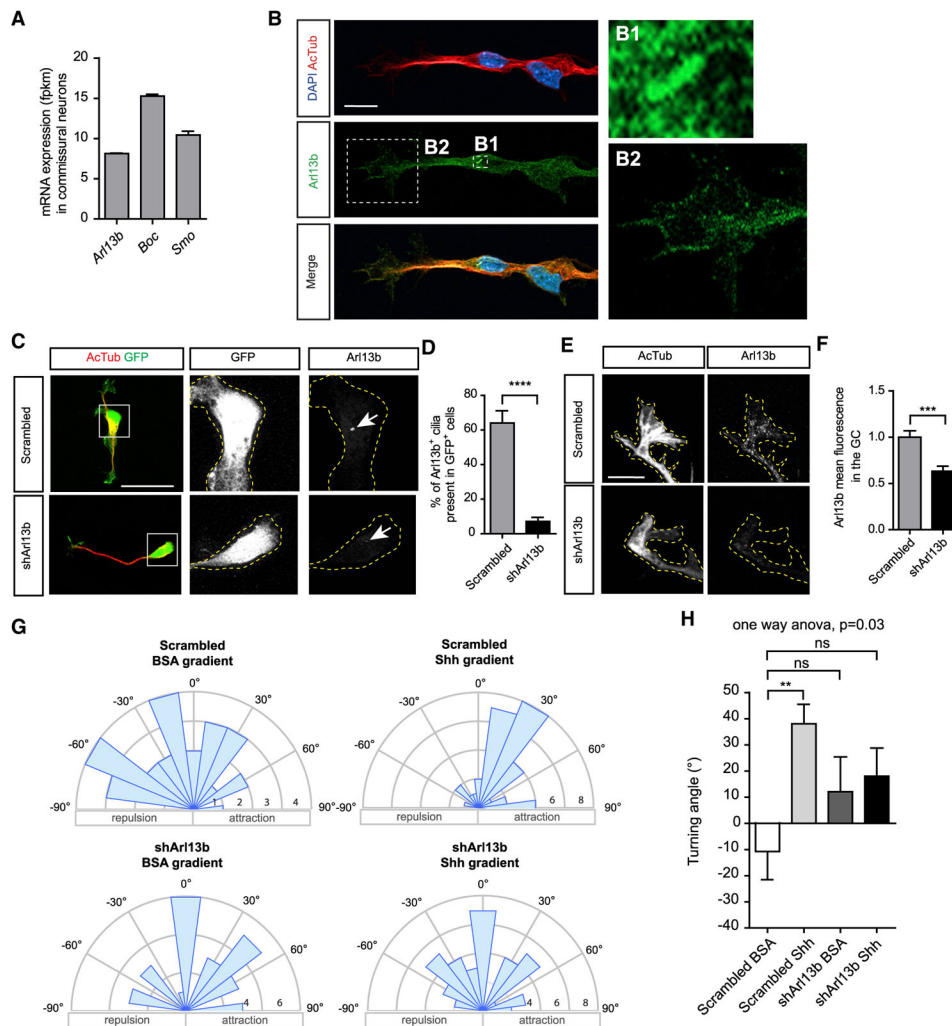
See also Figure S1.

Figure 3. Arl13b Is Required for Shh-Mediated Growth Cone Turning

(A) The mean mRNA expression (fragments per kilobase of exon per million reads [fpkm] ± SEM) of *Arl13b, Boc,* and *Smo* in dissociated commissural neurons (n = 3 independent experiments).

(B) Arl13b and acetylated tubulin immunostaining of dissociated commissural neurons. Arl13b is highly enriched at the primary cilium (zoom-in, B1) and present in the growth cone (zoom-in, B2).

(C) Arl13b immunostaining of neurons electroporated with scrambled shRNA or shRNA against Arl13b (shArl13b). Electroporated neurons were monitored by GFP expression.

(D) Quantification of the percentage of electroporated (GFP+) cells showing an Arl13b+ cilium (±SEM) compared to scrambled (Mann-Whitney test) (80 cells for scrambled and 77 cells for shArl13b).

(E) When shArl13b is electroporated in commissural neurons, the growth cone Arl13b staining is highly reduced.

(F) Quantification of Arl13b mean fluorescence in the growth cone (± SEM) compared to scrambled (Mann-Whitney test, n = 3 independent experiments).

(G) Rose histograms of the distribution of angles turned by commissural axons expressing either scrambled shRNA or shArl13b in Dunn chambers, exposed to a gradient of Shh (0.1 μg/ml) or BSA. Responses of individual neurons were clustered in 15° bins, and the number of neurons per bin is represented by the radius of each segment.

(H) Quantification of the angle turned (mean ± SEM) (one-way ANOVA, Dunnett's multiple comparison post-test, *$p < 0.05$, n > 30 neurons per condition).
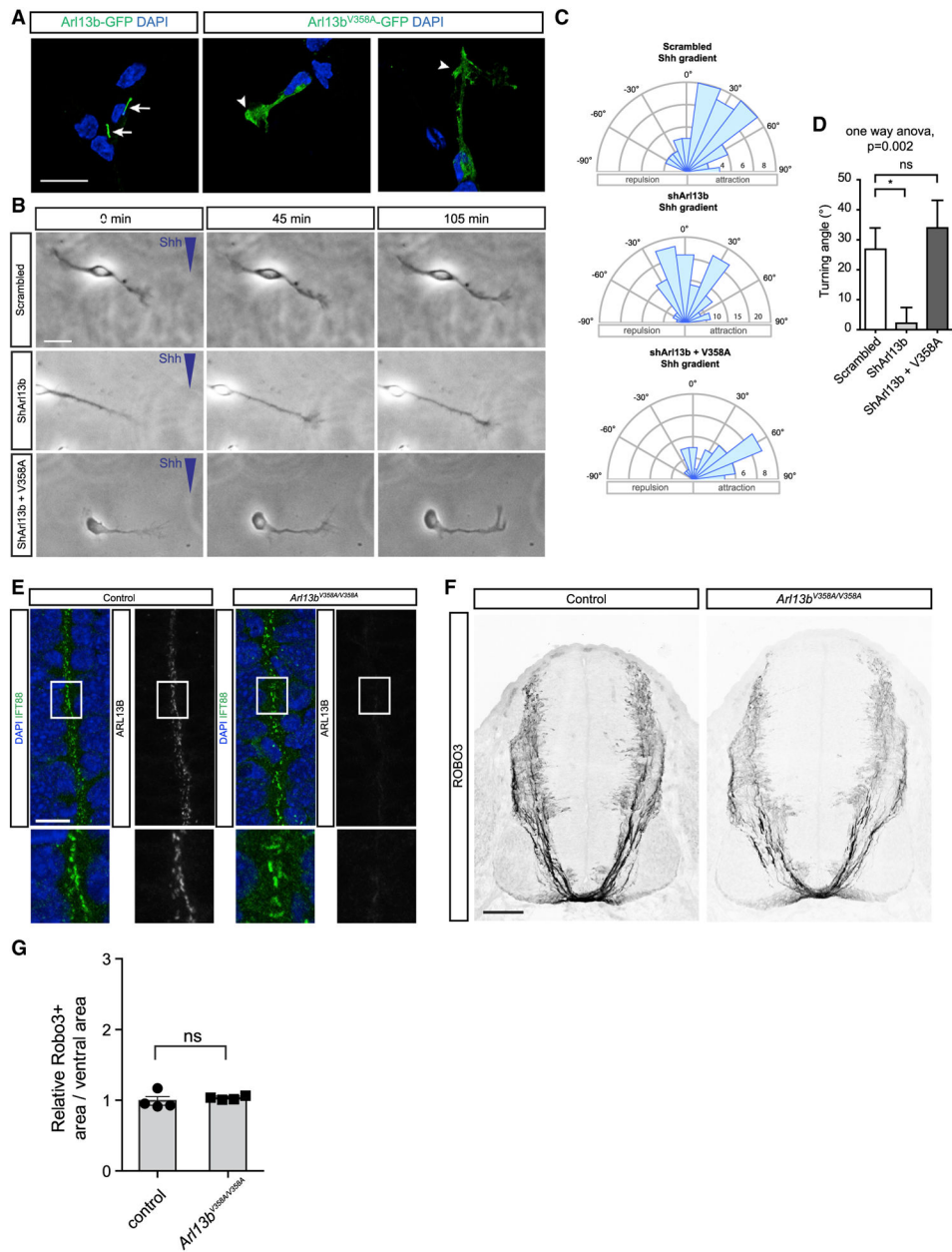
Scale bars: 10 μm (B), 20 μm (C), and 5 μm (E).

Figure 4. Cilia-Localization-Deficient Arl13b Is Sufficient for Shh-Mediated Growth Cone Turning *In Vitro* and Commissural Axon Guidance *In Vivo*

(A) Arl13b-GFP or Arl13b[V358A]-GFP localization in commissural neurons. Arrows: primary cilia. Arrowheads: growth cones.

(B) Commissural neurons expressing scrambled shRNA, shArl13b, or shArl13b + cilia-localization-deficient Arl13b (V358A) exposed to a gradient of Shh (0.1 μg/ml) or BSA.

(C and D) Rose histograms (C) or standard histogram (D) of the angle turned (mean ± SEM) (one-way ANOVA, Tukey's multiple comparison post-test, **$p < 0.01$, n > 30 neurons per condition).

(E) IFT88 and Arl13b co-immunostaining of E11.5 spinal cord cross-sections of *Arl13b[V358A/V358A]* mice compared to control mice.

(F) Robo3 immunostaining of E11.5 spinal cord cross-sections of *Arl13b^{V358A/V358A}* mice compared to control mice.

(G) Quantification of the area occupied by Robo3+ axons relative to the total area of the ventral neural tube (mean ± SEM) (t test). Number of embryos: 4 *Arl13b^{V358A/V358A}*; 4 control; and 2 sections per embryo.

Scale bars: 20 μm (A), 10 μm (B and E), and 200 μm (F).

See also Figures S2 and S3.

KEY RESOURCES TABLE

REAGENT or RESOURCE	SOURCE	IDENTIFIER
Antibodies		
Goat polyclonal anti-Robo3 (1:500 for IF)	R&D Systems	Cat#: AF3076; RRID: AB_2181865
Mouse anti-Shh 5E1 (1:20 for IF)	Developmental Studies Hybridoma Bank	Cat#: 5E1; RRID:AB_528466
Rabbit polyclonal anti-Arl13b (1:2000 for IF)	Caspary et al., 2007	N/A
Mouse anti-Arl13b (1:2000 for IF)	NeuroMab	Cat# N295B/66; RRID:AB_2750771
Rabbit polyclonal anti-IFT88 (1:1000)	kind gift from Brad Yoder	N/A
Mouse anti-Lhx2 (1:100 for IF)	Developmental Studies Hybridoma Bank	PCRP-LHX2-1C11; RRID:AB_2618817
Donkey anti-goat IgG Cy3 (1:500)	Jackson ImmunoResearch Laboratory	Cat#: 705-165-147; RRID: AB_2307351
Secondary antibodies were conjugated to Alexa Fluor 488, 568 or 594 (1:1000).	Thermo Fisher	Cat#: A21202; RRID:AB_141607, A10037; RRID:AB_2534013, A21206; RRID:AB_2535792, A21207; RRID:AB_141637
Bacterial and Virus Strains		
DH5a	Life Technologies	Cat#: 18265-017
*ccd*B	Thermo Fisher	Cat#: A10460
HB101	Promega	Cat#: L2011
Chemicals, Peptides, and Recombinant Proteins		
Recombinant Human Sonic Hedgehog (C24II) N terminus	R&D Systems	Cat#: 1845-SH
Bovine serum albumin (BSA)	MultiCell	500-0206
Poly-L-lysine solution (molecular weight 70,000-150,000, concentration: 0.01%)	Sigma-Aldrich	P4707
DAPI	Sigma-Aldrich	Cat# D9564
Critical Commercial Assays		
Primary Cell 96-well Nucleofector Kit	Lonza	Cat #: V4SP-3960
Experimental Models: Organisms/Strains		
Rat: ARS/Sprague Dawley	Charles River (St. Constant, Canada)	N/A
Arl13b^{hennin}	Caspary et al., 2007	MGI:3578151
Tulp3$^{tm1b(EUCOMM)hmgu}$	Legue and Liem, 2019	MGI: 5548429
Kif7	Cheung et al., 2009	MGI:4357956
Arl13b^{V358A}	Gigante et al., 2019	MGI:6256969
Recombinant DNA		
pcDNA6.2-GW/EmGFP-miR	Invitrogen	K493600
pCAGGs-mouse Arl13b-GFP	This article	N/A
pDONR221	ThermoFisher	12536-017
pcDNA-DEST47	ThermoFisher	12281-010
pCAGGS	Stühmer et al., 2002	N/A
pCAGGS-Arl13b^{Y86C}-GFP	This article	N/A
pCAGGS-Arl13b^{R79Q}-GFP	This article	N/A

REAGENT or RESOURCE	SOURCE	IDENTIFIER
pCAGGS-Arl13b^{R200C}-GFP	This article	N/A
Software and Algorithms		
Prism 7 for Mac OS X	Graphpad	https://download.cnet.com/GraphPad-Prism/3000-2053_4-8453.html
ImageJ	NIH	https://imagej.nih.gov/ij/
BLOCK-iT_ RNAi Designer	ThermoFisher Scientific	https://rnaidesigner.thermofisher.com/rnaiexpress/
Illustrator CC	Adobe	http://www.adobe.com/jp/products/illustrator.html
Photoshop CC	Adobe	https://www.adobe.com/products/photoshop.html
Other		
Dunn Chamber	Hawksley	DC-100